

Detailed abundances of Red Giants in the Globular Cluster NGC 1851: C+N+O and the Origin of Multiple Populations

S. Villanova and D. Geisler

Departamento de Astronomía, Casilla 160, Universidad de Concepción, Chile

svillanova@astro-udec.cl

and

G. Piotto

Dipartimento di Astronomia, Università di Padova, Vicolo dell'Osservatorio 3, I-35122 Padua, Italy

ABSTRACT

We present chemical abundance analysis of a sample of 15 red giant branch (RGB) stars of the Globular Cluster NGC 1851 distributed along the two RGBs of the $(v, v-y)$ CMD. We determined abundances for C+N+O, Na, α , iron-peak, and s-elements. We found that the two RGB populations significantly differ in their light (N,O,Na) and s-element content. On the other hand, they do not show any significant difference in their α and iron-peak element content. More importantly, the two RGB populations do not show any significant difference in their total C+N+O content.

Our results do not support previous hypotheses suggesting that the origin of the two RGBs and the two subgiant branches of the cluster is related to a different content of either α (including Ca) or iron-peak elements, or C+N+O abundance, due to a second generation polluted by SNeII.

Subject headings: globular clusters: general — globular clusters: individual(NGC 1851)

1. Introduction

Recent investigations have fostered new interest in globular cluster (GC) stellar populations. The traditional vision of GCs hosting simple, single age, single metallicity stars has been shattered by the discovery of multiple sequences in the color-magnitude diagrams (CMD) and of large dispersions in light or heavy element abundances, often showing well defined patterns, which are the result of nuclear processes in a previous generation of stars.

NGC 1851 is one of the GCs where multiple stellar populations have been clearly identified. Indeed, in recent years, this GC has been the subject of a wide photometric and spectroscopic observational campaign. First of all, Milone et al. (2008) have identified a double subgiant branch (SGB) in the cluster CMD, clearly suggesting the

presence of at least two stellar generations. As discussed by Milone et al. (2008), if the SGB split would be due to a different age between the two populations with similar metal content, the second generation of stars should have formed ~ 1 Gyr after the first one. However other factors could be at work. As pointed out by Cassisi et al. (2008) and Ventura et al. (2009), the SGB splitting could also be explained by a difference in the total C+N+O content, with an abundance for the fainter SGB 2-3 times larger than that of the brighter one. In this case, the age spread would be smaller, of the order of a few hundred Myrs.

Unfortunately, we have scarce information on detailed abundances of NGC 1851 stars. Hesser et al. (1982) collected low resolution spectra for 18 stars. They found a constant iron content, but 3 out of 8 of their bright RGB stars show anomalously strong CN bands. More re-

cently, Yong & Grundahl (2008) analyzed UVES spectra of eight giants. With all the limitations coming from the small number statistics, Yong & Grundahl (2008) results seem to indicate the presence of a Na-O anticorrelation, and the presence of a large star to star abundance scatter of s-process elements Zr and La, with some hints of a bimodal distribution. They also find a large star to star variation in the strength of the Ba lines. They also show that the split of the RGB found by Calamida et al. (2007) in a Strömgren photometry CMD is related to the double SGB. Interestingly, the fraction of La/Zr-strong stars (40%) is tantalizingly similar to the fraction of SGB-faint stars (45%), and to the fraction of the CN-strong, Ba-strong, and Sr-strong RGB stars (40%) of Hesser et al. (1982). But the sample statistics for stars with abundance estimates is very poor. Recently, Yong et al. (2009) suggested the presence of a large C+N+O spread (~ 0.6 dex) among NGC 1851 giant stars. Their work is based on high resolution spectra of four stars. This spread could imply that one population has 4 times larger C+N+O content with respect to the other, supporting the scenario proposed by Cassisi et al. (2008) and Ventura et al. (2009). However, also in this case, the statistics is very poor.

In order to account for such observational results, it has been proposed that a second generation of stars may have formed from a residual reservoir of gas polluted by intermediate mass asymptotic giant branch (AGB) star ejecta (D’Antona et al. 2002), or from the ejecta of massive fast rotating stars (Decressin et al. 2007). A very recent work by Lee et al. (2009) proposes another possibility. Using Strömgren photometry and the Ca narrow-band filter centered on the H-K Ca lines at ~ 3950 Å, Lee et al. (2009) find a significant color split in the RGB of many clusters, including NGC 1851. Because of the observed split, Lee et al. (2009) propose that the two RGBs have a different Ca content, of the order of 0.3 dex. In this case, the second generation of stars could originate from gas polluted by SNeII explosions, the only mechanism able to produce a Ca enhancement. However, this scenario is quite controversial, because multiple CMD sequences have been found in other clusters, where abundances based on high resolution spectra give a negligible or very low Ca spread. For exam-

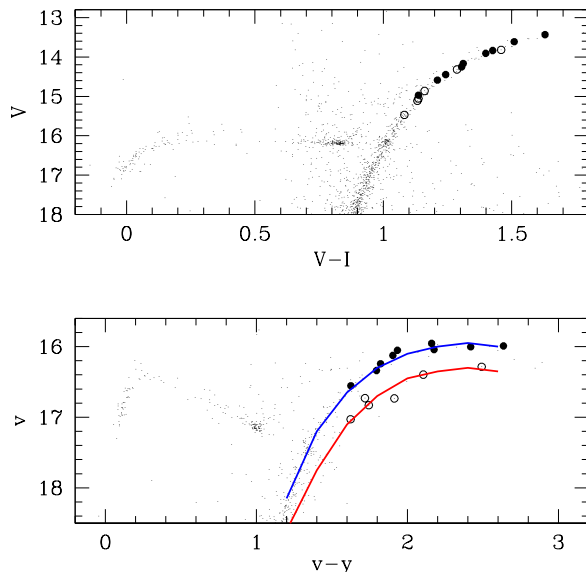


Fig. 1.— V vs. V-I and v vs. v-y CMDs of our target stars. The double RGB is visible in the v vs. v-y CMD but not in the V vs. V-I CMD. The blue RGB is indicated as a blue line, the red RGB as a red line. Ba-poor stars are plotted as filled circles, while Ba-rich as open circles.

ple, there is the case of M4, where Marino et al. (2008) and Carretta et al. (2010a) found no Ca spread at all, while Lee et al. (2009) presented a CMD with a double RGB. In M4, a clear RGB spread is visible in ultraviolet broad-band photometry (see Fig. 11 of Marino et al. (2008)), but, as discussed in Marino et al. (2008), the photometric spread can be better explained by a spread in C,N,O.

The only way to solve the enigma is to measure C,N,O, α , iron-peak, and s-process element abundances for a statistically significant sample of RGB stars. For this purpose we observed a sample of 15 RGB stars distributed among the two RGBs of the Strömgren (v,v-y) CMD with high and medium resolution spectroscopy. The observations, data reduction, chemical abundance analysis, and results will be presented in the following sections.

In this letter we discuss only the results on Fe, Ca, s-process, and C+N+O content, i.e. the most

relevant elements in the context of the present debate on multiple stellar populations in GCs. Full details will be presented in a subsequent paper.

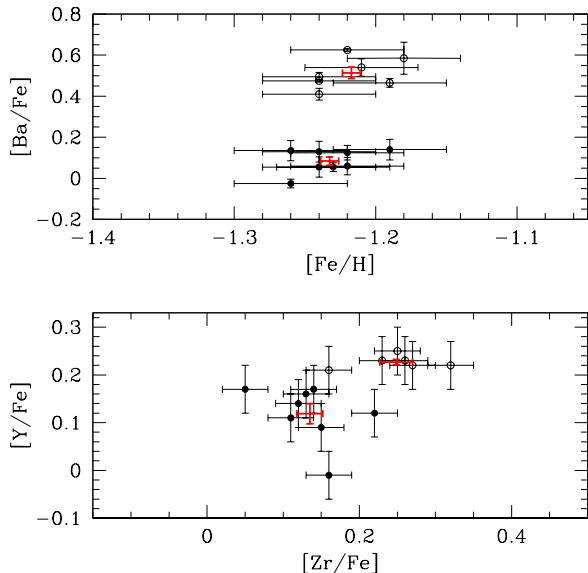


Fig. 2.— $[\text{Ba}/\text{Fe}]$ vs. $[\text{Fe}/\text{H}]$ and $[\text{Y}/\text{Fe}]$ vs. $[\text{Zr}/\text{Fe}]$ for our target stars. Ba-poor stars are plotted as filled circles, while Ba-rich as open circles. Red crosses give mean values and errors of the mean for the two groups of stars.

2. Observations

Our dataset consists of high and medium resolution spectra collected in November-December 2008. The spectra come from single ~ 1500 and ~ 500 s exposures, obtained with the MIKE and Mage slit spectrographs¹ respectively, mounted at the Magellan/Clay telescope. Weather conditions were excellent with a typical seeing of 0.5 arcsec. We selected 15 isolated stars from 0.5 magnitudes above the RGB-bump to the tip of the RGB, in the magnitude range $15.5 < V < 13.5$. The MIKE spectra have a spectral coverage from 4900 to 8700 \AA with a resolution of ~ 32000 and $\text{S/N} > 100$ at 6300 \AA . The Mage spectra have a spectral coverage from 3700 to 9500 \AA with a resolution of ~ 5000 and $\text{S/N} > 50$ at 4300 \AA .

¹See www.lco.cl

Data were reduced using IRAF² including bias subtraction, flat-field correction, wavelength calibration, scattered-light and sky subtraction, and spectral rectification.

In the case of MIKE observations, spectra were corrected for fringing using the spectrum of a hot fast rotating star, which gave the best result compared with other methods. However, fringing did not affect the spectral region we were interested in (below 8100 \AA).

Targets were carefully selected in order to have stars in each of the two distinct RGBs clearly separated in the high quality v vs. $v-y$ Strömgen photometry CMD (see Fig. 1, lower panel) kindly provided by F. Grundahl. In the following, we used also VI Cousins photometry from Y. Momany. Note that there is no RGB split in the V vs. $V-I$ CMD (Fig. 1, upper panel). Filled and open circles in Fig. 1 are Ba-poor and Ba-rich stars, respectively (as measured from our spectra, see Sec. 4). All stars were observed with both spectrographs.

Radial velocities were measured by the *fxcor* package in IRAF, using a synthetic spectrum as a template. The mean heliocentric value for our targets is 320.3 ± 1.1 km/s, while the dispersion is 4.4 ± 0.8 km/s. Harris (1996) gives 320.5 ± 0.6 km/s as heliocentric radial velocity for NGC1851, and the typical dispersion for a cluster of its mass is $\sim 4-5$ km/s (Pryor & Meylan 1993). All our targets have a radial velocity within ± 15 km/s of the cluster radial velocity. On the basis of this result, we conclude that all our targets are cluster members.

3. Abundance analysis

The chemical abundances for Na, Si, Ca, Ti, Fe, and Ni were obtained from the equivalent widths (EWs) of the spectral lines. See Marino et al. (2008) for a more detailed explanation of the method we used to measure the EWs and for the adopted solar abundances. For the other elements (C, N, O, Y, Zr, Ba), whose lines are affected by blending, we used the spectral synthesis method. Na presents few features in the spectrum, so in

²IRAF is distributed by the National Optical Astronomy Observatory, which is operated by the Association of Universities for Research in Astronomy, Inc., under cooperative agreement with the National Science Foundation

this case abundances derived from the EWs were cross-checked with the spectral synthesis method in order to obtain more accurate measurements. MIKE spectra were used to obtain abundances for all the elements but C, which was obtained from Mage data. Only lines not contaminated by telluric lines were used.

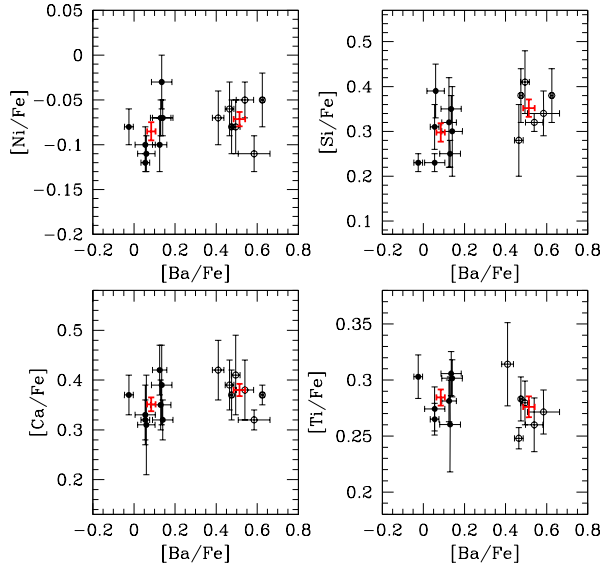


Fig. 3.— Ni and α -element abundances of our target stars. Ba-poor stars are plotted as filled circles, while Ba-rich as open circles. Red crosses are mean values and errors of the mean for the two groups of stars.

Atmospheric parameters were obtained in the following way. First of all T_{eff} was derived from the V-I color using the relation by Alonso et al. (1999) and the reddening from Harris (1996). Surface gravities ($\log(g)$) were obtained from the canonical equation:

$$\log\left(\frac{g}{g_{\odot}}\right) = \log\left(\frac{M}{M_{\odot}}\right) + 4 \cdot \log\left(\frac{T_{\text{eff}}}{T_{\odot}}\right) - \log\left(\frac{L}{L_{\odot}}\right)$$

where the mass M/M_{\odot} was derived from isochrone fitting using the Padova database (Marigo et al. 2008), and the luminosity L/L_{\odot} was obtained from the absolute magnitude M_V assuming an apparent distance modulus of $(m - M)_V = 15.47$ (Harris 1996). The bolometric correction (BC) was derived by adopting the relation BC- T_{eff} from

Alonso et al. (1999). Finally, microturbulence velocity (v_t) was obtained from the relation of Gratton et al. (1996).

These atmospheric parameters were considered as initial estimates and were refined during the abundance analysis. As a first step atmospheric models were calculated using ATLAS9 (Kurucz 1970) and assuming the initial estimate of T_{eff} , $\log(g)$, and v_t , and the $[\text{Fe}/\text{H}]$ value from Harris (1996).

Then T_{eff} , v_t , and $\log(g)$ were adjusted and new atmospheric models calculated in an interactive way in order to remove trends in Excitation Potential (E.P.) and equivalent widths vs. abundance for T_{eff} and v_t respectively, and to satisfy the ionization equilibrium for $\log(g)$. FeI and FeII were used for this purpose. The $[\text{Fe}/\text{H}]$ value of the model was changed at each iteration according to the output of the abundance analysis.

The Local Thermodynamic Equilibrium (LTE) program MOOG (Snedden 1973) was used for the abundance analysis.

We checked the reliability of our atmospheric parameters in the following way. Intrinsic V-I colours of our stars were obtained from our T_{eff} by inverting the Alonso et al. (1999) equation. Comparing intrinsic and measured colours we got a reddening of $E(B-V) = 0.01 \pm 0.01$ (assuming $E(V-I) = 1.24 \times E(B-V)$).

This value is in very good agreement with Harris (1996), that gives $E(B-V) = 0.02$.

A further check to test the reliability of our T_{eff} and $\log(g)$ values was performed on Arcturus, which is an important reference for every study on RGB stars.

In order to have statistically independent estimations, we measured the atmospheric parameters on 3 high-resolution high-S/N spectra obtained with HARPS, the high precision spectrograph mounted at the 3.6m telescope in La Silla.

We obtained $T_{\text{eff}} = 4290 \pm 11$ K and $\log(g) = 2.00 \pm 0.02$ as mean values and internal errors, which agree extremely well with literature values ($T_{\text{eff}} = 4290 \pm 30$ K, $\log(g) = 1.9 \pm 0.1$, Griffin & Lynas-Gray 1999).

Our conclusion is that our T_{eff} and $\log(g)$ scales appear free from significant systematic errors.

The linelists for the chemical analysis were obtained from many sources (Gratton et al. (2003),

VALD & NIST³, McWilliam et al. (1994), McWilliam (1998), SPECTRUM⁴, and SCAN⁵), and calibrated using the Solar-inverse technique by the spectral synthesis method. For this purpose we used the high resolution, high S/N NOAO Solar spectrum (Kurucz et al. 1984). For Ba lines we took the hyperfine splitting into account. We emphasize the fact that all the linelists were calibrated on the Sun, including those used for the spectral synthesis.

In particular, our determinations of C,N,O abundances are based on the G-band at 4310 Å, the CN lines at 8003 Å, and the forbidden O line at 6300 Å respectively. CN lines at 8003 Å were used also to estimate the C¹²/C¹³ ratio.

For the Sun we have $\log\epsilon(\text{C})=8.49$, $\log\epsilon(\text{N})=7.95$, and $\log\epsilon(\text{O})=8.83$, values that agree with Grevesse & Sauval (1998) within 0.03 dex.

These three features were also checked on the high resolution, high S/N spectrum of Arcturus by Hinkle et al. (2003) in order to verify if further blends affecting cool RGB stars but not the Sun were present. We found no significant contamination.

We obtained the following results for Arcturus: $[\text{C}/\text{Fe}]=-0.10\pm 0.05$, $[\text{N}/\text{H}]=+0.34\pm 0.05$, $[\text{O}/\text{Fe}]=+0.38\pm 0.05$ (internal errors). These values well agree with Peterson et al. (1993), which gives $[\text{C}/\text{Fe}]=+0.0\pm 0.1$, $[\text{N}/\text{H}]=+0.3\pm 0.1$, $[\text{O}/\text{Fe}]=+0.4\pm 0.1$. We consider this as a test which proves the reliability of our linelists for C,N,O not only on Sun-like stars, but also on cool RGB stars.

Abundances for C, N, and O were determined all together in an interactive way, because for the temperature of our stars, carbon, nitrogen, and oxygen form molecules and as a consequence their abundances are related to each other.

Our C¹²/C¹³ estimation (C¹²/C¹³<15 for all our targets) confirm that the stars are affected by evolutionary mixing, as expected from their position in the CMD. This can affect the primordial C,N,O abundances separately, but not the total C+N+O content because these elements are transformed one into the other during the CNO cycle.

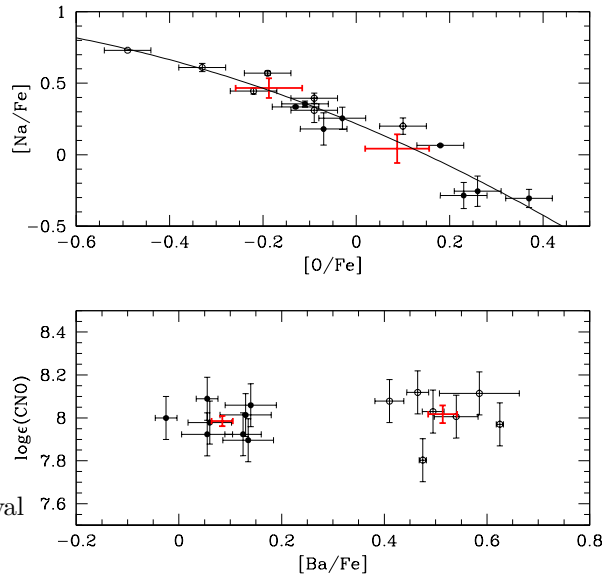


Fig. 4.— Na-O anticorrelation and CNO abundances for our targets. Ba-poor stars are plotted as filled circles, while Ba-rich as open circles. Red crosses are mean values and errors of the mean for the two groups of stars.

4. Results and Discussion

First of all, in Fig. 2 we plot the abundance of Ba vs. Fe. (upper panel). In this plot we clearly see that the Ba distribution is bimodal, while the iron abundance for the two Ba groups is the same within the errors. In the following analysis, we divided our stars into two groups, one Ba-poor (filled circles in the figures), and the other Ba-rich (open circles).

The individual and mean abundances we obtained for the two groups are summarized in Tab. 1. For the mean abundances we reported also the internal errors (standard deviation of the mean).

The two groups have:

$$[\text{Fe}/\text{H}]=-1.23\pm 0.01, [\text{Ba}/\text{Fe}]=+0.08\pm 0.02$$

and

$$[\text{Fe}/\text{H}]=-1.22\pm 0.01, [\text{Ba}/\text{Fe}]=+0.51\pm 0.03$$

as mean values respectively. The lower panel of Fig. 2 displays the abundances of two other s-

³See <http://vald.astro.univie.ac.at/~vald/php/vald.php> and http://physics.nist.gov/PhysRefData/ASD/lines_form.html

⁴See <http://www.phys.appstate.edu/spectrum/spectrum.html> and references therein

⁵See <http://www.astro.ku.dk/~uffegj/>

TABLE 1

ABUNDANCES OF THE TWO GROUPS OF STARS. MEAN ABUNDANCES OF THE TWO POPULATIONS AND THE RELATED INTERNAL ERRORS ARE REPORTED AT THE BOTTOM OF THE TABLE. ERRORS ASSOCIATED WITH THE MEASUREMENTS ARE PLOTTED IN FIGS. 2,3, AND 4.

Id	[Fe/H]	[Ba/Fe]	[Zr/Fe]	[Y/Fe]	[Ni/Fe]	[Si/Fe]	[Ca/Fe]	[Ti/Fe]	[Na/Fe]	[O/Fe]	C+N+O
Ba-poor stars											
13	-1.24	0.06	0.16	-0.01	-0.10	0.23	0.33	0.27	-0.26	0.26	7.92
30	-1.23	0.06	0.05	0.17	-0.12	0.31	0.32	0.26	0.06	0.18	8.09
31	-1.26	-0.02	0.11	0.11	-0.08	0.23	0.37	0.30	-0.31	0.37	8.00
43	-1.22	0.06	0.14	0.17	-0.11	0.39	0.31	-	0.34	-0.13	7.98
51	-1.19	0.14	0.22	0.12	-0.07	0.30	0.32	0.30	0.26	-0.03	8.06
53	-1.22	0.13	0.15	0.09	-0.10	0.32	0.42	0.28	-0.28	0.23	7.92
63	-1.26	0.14	0.12	0.14	-0.03	0.35	0.39	0.31	0.18	-0.07	7.90
68	-1.24	0.13	0.13	0.16	-0.07	0.25	0.35	0.26	0.36	-0.11	8.01
Ba-rich stars											
35	-1.24	0.48	0.26	0.23	-0.08	0.38	0.37	0.28	0.31	-0.09	7.80
14	-1.21	0.54	0.32	0.22	-0.05	0.32	0.38	0.26	0.20	0.10	8.01
16	-1.24	0.50	0.16	0.21	-0.08	0.41	0.41	0.28	0.40	-0.09	8.03
18	-1.19	0.47	0.25	0.25	-0.06	0.28	0.39	0.25	0.73	-0.49	8.12
20	-1.24	0.41	0.23	0.23	-0.07	-	0.42	0.31	0.57	-0.19	8.08
8	-1.18	0.59	0.27	0.22	-0.11	0.34	0.32	0.27	0.44	-0.22	8.11
9	-1.22	0.63	-	-	-0.05	0.38	0.37	-	0.61	-0.33	7.97
Mean abundances and internal errors											
Ba-poor	-1.23	+0.09	+0.14	+0.12	-0.09	+0.30	+0.35	+0.28	+0.04	+0.09	7.99
	± 0.01	± 0.02	± 0.02	± 0.02	± 0.01	± 0.02	± 0.01	± 0.01	± 0.10	± 0.07	± 0.02
Ba-rich	-1.22	+0.52	+0.25	+0.23	-0.07	+0.35	+0.38	+0.28	+0.47	-0.19	8.02
	± 0.01	± 0.03	± 0.02	± 0.01	± 0.01	± 0.02	± 0.01	± 0.01	± 0.07	± 0.07	± 0.04

elements: Y and Zr. Again the two groups of Ba-rich and Ba-poor stars are separated, in the sense that the Y and Zr content is significantly different for Ba-poor and Ba-rich stars. The two groups have $[Zr/Fe]=+0.14\pm 0.02$, $[Y/Fe]=+0.12\pm 0.02$ and $[Zr/Fe]=+0.25\pm 0.02$, $[Y/Fe]=+0.23\pm 0.01$ respectively. The results displayed in the lower panel of Fig. 2 can be considered as an independent confirmation of the presence of two groups of stars with different s-element content in NGC 1851.

An interesting result comes from Fig. 1 (lower panel) which clearly shows that all Ba-poor stars are located in the bluer RGB, while all Ba-rich stars are located in the redder one. The two sequences seem to be well separated. As in the case of M22 (Marino et al. 2009), our result implies that s-elements allow us define two distinct populations also in NGC1851.

Now, it is instructive to analyze the α -element content of the two groups. We included in this analysis also Ni, another iron-peak element. For this purpose, we plot in Fig. 3 Ni vs. Ba (upper-left panel), Si vs. Ba (upper-right panel), Ca vs. Ba (lower-left panel), and Ti vs. Ba (lower-right panel).

The average value of Ni, Si, Ca, and Ti for the two different Ba groups is summarized in Table 1, with the corresponding internal dispersion of the mean plotted in the figure. As already found for iron (Fig. 2), the Ba-rich and Ba-poor groups have no appreciable difference in their iron-peak element and α -element content, which have similar values within $1-1.5\sigma$.

This result is in contrast with the hypothesis by Lee et al. (2009), and consistent with Carretta et al. (2010a)'s statement that most GCs do not have an appreciable spread in their iron-peak or α -element content. Our results also imply that in the case of NGC1851 pollution by SNeII cannot explain the double population.

As for the lighter elements, Fig. 4 (upper panel) confirms that the cluster has a very well defined Na-O anticorrelation, as already shown by Yong & Grundahl (2008).

However, here we have an interesting new result. The two Ba groups are partially separated in the Na vs. O plot, with some overlap at $-0.1 < [O/Fe] < +0.1$. Ba-poor stars have an aver-

age $[Na/Fe]=+0.04\pm 0.10$ and $[O/Fe]=+0.09\pm 0.07$, while Ba-rich stars have $[Na/Fe]=+0.47\pm 0.07$, $[O/Fe]=-0.19\pm 0.07$.

We found that Na is correlated also with C and N. The two groups of stars have different mean N contents ($[N/Fe]=1.09\pm 0.08$ dex for Ba-poor stars, $[N/Fe]=0.73\pm 0.16$ for Ba-rich stars, but very similar mean C content ($[C/Fe]=-0.64\pm 0.09$ dex for Ba-poor stars, $[C/Fe]=-0.72\pm 0.08$ for Ba-rich stars). However, as in the case of M22, C, N and O do not show a bimodal distribution (Villanova et al., in preparation). How C,N,O content is related to the double RGB visible in the (v, v-y) CMD is not clear. We know that the v band contains many CH and CN features which, according to Marino et al. (2008), can contribute to split the RGB in UV or blue CMDs. CH bands affect also the Ca narrow-band filter used by Lee et al. (2009), and this could explain their RGB split without invoking a Ca spread.

Any interpretation of the CMD and of the spectroscopic results involving C,N,O should also take into account the evolutionary stage of our targets. The investigation of light-element correlations and the relation between the double RGB and the C,N,O content is beyond the scope of this letter and will be discussed in detail in a future paper.

Our final interesting result concerns C+N+O. Fig. 4 (lower panel) shows that the two groups of stars have the same C+N+O content, within 1σ . In particular, the Ba-poor group have $\log\epsilon(CNO)=7.99\pm 0.02$, while the Ba-rich have $\log\epsilon(CNO)=8.02\pm 0.04$.

About the mean C12/C13 content of the two populations we found they have the same values (~ 5) within the errors. We expected the Ba-rich stars to have a lower C12/C13 value as the results of the contamination of the pristine gas they formed from by highly processed ejecta.

However we point out that our results about C12/C13 are preliminar. Also the evolutionary stage of the targets must be taken into account, which could alter the primordial mean C12/C13 ratio of the two populations making them to assume a similar value.

A better estimation of C12/C13 for each targets and a theoretical treatment of the expected difference between the two population will be presented in a future paper.

Figure 4 excludes the possibility that the second

generation of stars have a significantly enhanced C+N+O content, as suggested by Cassisi et al. (2008), Ventura et al. (2009), and Yong et al. (2009). Unfortunately we do not have stars in common with Yong et al. (2009) for a comparison. Here we note that Yong et al. (2009) targets are very bright, close to the RGB-tip. It is well possible that some of their stars are indeed AGB stars. In such a case, the chemical pattern shown by those stars may have been highly altered by internal nuclear processes.

However, as suggested by Cassisi et al. (2008), if the first generation had $\log\epsilon(\text{CNO})=8.00$ dex, then a second generation with double C+N+O content would correspond to $\log\epsilon(\text{CNO})=8.30$ dex. At odd with that, a difference in $\log\epsilon(\text{CNO})$ of 0.03, as we find, implies that the Ba-rich population have about 1.1 times the C+N+O content of the Ba-poor one, which is consistent with a null difference when we consider the measurement errors.

The dichotomy in Ba and other s-process element content, as well as the clear spread in the CMD of Fig. 1 clearly points towards the presence of two distinct stellar populations in NGC 1851, as found also by Milone et al. (2008) in the SGB. However, the constancy of the CNO content casts doubts on the scenario of a second population born from material polluted by first generation intermediate mass stars. The possibility of a merge of two distinct clusters, as very recently suggested by Carretta et al. (2010b) should be further explored.

S.V. and D.G. acknowledge the support by BASAL/ FONDAP project.

G.P. acknowledges the support by MIUR under the program PRIN2007 (prot. 20075TP5K9).

The author acknowledge F. Grundahl and Y. Momany which kindly provided the photometry.

REFERENCES

- Alonso, A., Arribas, S., & Martínez-Roger, C. 1999, *A&AS*, 140, 261
- Calamida, A., Bono, G., Stetson, P.B., Freyhammer, L.M., Cassisi, S., Grundahl, F., Pietrinferni, A., Hilker, M., Primas, F., & Richtler, T. 2007, *ApJ*, 670, 400
- Carretta, E., Bragaglia, A., Gratton, R., Lucatello, S., Bellazzini, M., & D’Orazi, V. 2010, arXiv:1002.0002
- Carretta, E., Gratton, R.G., Lucatello, S., Bragaglia, A., Catanzaro, G., Leone, F., Momany, Y., D’Orazi, V., Cassisi, S., D’Antona, F., & Ortolani, S. 2010, arXiv1007.5301C
- Cassisi, S., Salaris, M., Pietrinferni, A., Piotto, G., Milone, A.P., Bedin, L.,R., & Anderson, J. 2008, *ApJ*, 672, 115
- D’Antona, F., Caloi, V., Montalbán, J., Ventura, P., & Gratton, R. 2002, *A&A*, 395, 69
- Decressin, T., Meynet, G., Charbonnel, C., Prantzos, N., & Ekström, S. 2007, *A&A*, 464, 1029
- Gratton, R.G., Carretta, E., & Castelli, F. 1996, *A&A*, 314, 191
- Gratton, R.G., Carretta, E., Claudi, R., Lucatello, S., & Barbieri, M. 2003, *A&A*, 404, 187
- Grevesse, N., & Sauval, A.J. 1998, *SSRv*, 85, 161
- Griffin, R.E.M., & Lynas-Gray, A.E. 1999, 1999, *AJ*, 117, 2998
- Harris, W.E. 1996, *AJ*, 112, 1487
- Hesser, J.E., Bell, R.A., Harris, G.L.H., & Cannon, R. D. 1982, *AJ*, 87, 1470
- Hinkle, K., Wallace, L., Livingston, W., Ayres, T., Harmer, D., & Valenti, J. 2003, *csss*, 12, 851
- Kurucz, R.L. *SAO*, 309
- Kurucz, R.L., Furenlid, I., Brault, J., & Testerman, L. 1984, Solar flux atlas from 296 to 1300 nm, National Solar Observatory Atlas, Sunspot, New Mexico: National Solar Observatory
- Kurucz, R.L. *IAU Symp.*, 149, 225
- Lee, J.W., Lee, J., Kang, Y.W., Lee, Y.W., Han, S.I., Joo, S.J., Rey, S.C., & Yong, D. 2009, *ApJ*, 695, 78
- Marigo, P., Girardi, L., Bressan, A., Groenewegen, M. A. T., Silva, L., & Granato, G. L. 2008, *A&A*, 482, 883
- Marino, A.F., Villanova, S., Piotto, G., Milone, A.P., Momany, Y., Bedin, L.R., & Medling, A.M. 2008, *A&A*, 490, 625

- Marino, A. F., Milone, A. P., Piotto, G., Villanova, S., Bedin, L. R., Bellini, A. & Renzini, A. 2009, *A&A*, 505, 1099
- McWilliam, A., & Rich, R.M. 1994, *ApJS*, 91, 749
- McWilliam, A. 1998, *AJ*, 115, 1640
- Milone, A.P., Bedin, L.R., Piotto, G., Anderson, J., King, I.R., Sarajedini, A., Dotter, A., Chaboyer, B., Marín-Franch, A., Majewski, S. 2008, *ApJ*, 673, 241
- Peterson, R.C., Dalle Ore, C.M., & Kurucz, R.L. 1993, *ApJ*, 404, 333
- Pryor, C., & Meylan, G. 1993, *Structure and Dynamics of Globular Clusters*, ed. S.G. Djorgovski, & G. Meylan, *ASP Conf. Ser.*, 50, 357
- Sneden, C. 1973, *ApJ*, 184, 839
- Yong, D., & Grundahl, F. 2008, *ApJ*, 672, 29
- Yong, D., Grundahl, F., D'Antona, F., Karakas, A.I., Lattanzio, J.C., & Norris, J.E. 2009, *ApJ*, 695, 62
- Ventura, P., Caloi, V., D'Antona, F., Ferguson, J., Milone, A., & Piotto, G.P. 2009, *MNRAS*, 399, 934